Article

J. Biol. Regul. Homeost. Agents. 2024; 38(5): 4021–4036
https://doi.org/10.23812/j.biol.regul.homeost.agents.20243805.318

Inhibition of *DNMT3B* Suppresses the Proliferation and Migration of Oral Squamous Cell Carcinoma Cells through the Regulation of *GPX3* Expression

Ruifeng Zhu[1], Xianzhi Xu[1], Yiting Mao[1], Yingying Li[1], Jiwei Zheng[1,2,*]

[1]School of Stomatology, Xuzhou Medical University, 221004 Xuzhou, Jiangsu, China
[2]Department of Oral and Maxillofacial Surgery, Affiliated Hospital of Xuzhou Medical University, 221000 Xuzhou, Jiangsu, China
*Correspondence: zhengjiwei_zhjw@163.com (Jiwei Zheng)
Published: 1 May 2024

Background: DNA (cytosine-5-)-methyltransferase 3 beta (*DNMT3B*) can promote the development of oral squamous cell carcinoma (OSCC), while glutathione peroxidase 3 (*GPX3*) can inhibit it. In this study, we aimed to investigate the underlying mechanism by which *DNMT3B* and *GPX3* influence OSCC.

Methods: Bioinformatics was used to analyze the expression patterns of *DNMT3B* and *GPX3* in head and neck squamous cell carcinoma (HNSC), as well as the methylation sites in the promoter region of *GPX3*. Additionally, various cellular assays were conducted to assess the proliferation, migration, invasion, and apoptosis of OSCC cells including colony formation, Transwell®, and flow cytometry analyses. The levels of *DNMT3B*, *GPX3*, and factors related to the Jun N-terminal kinase (JNK)/c-JUN axis were quantified using quantitative real-time polymerase chain reaction (qRT-PCR) and Western blot. The methylation of the *GPX3* promoter and the interaction between *DNMT3B* and the *GPX3* promoter were evaluated through quantitative methylation-specific PCR and chromatin immunoprecipitation-PCR assays.

Results: The analysis revealed elevated expression of *DNMT3B* and reduced expression of *GPX3* in HNSC. Additionally, methylation sites were identified in the promoter region of the *GPX3* gene. Further investigation demonstrated that silencing *DNMT3B* suppressed the proliferation, migration, and invasion of OSCC cells while promoting apoptosis. This was accompanied by an increase in *GPX3* level and dephosphorylation of the JNK and c-JUN signaling pathways. *DNMT3B* was found to directly bind to the promoter of the *GPX3* gene. Overexpression of *GPX3* inhibited the proliferation, migration, and invasion of OSCC cells and promoted apoptosis. It also suppressed the JNK/c-JUN pathway. Conversely, silencing *GPX3* had the opposite effects and counteracted the effects of *DNMT3B* silencing.

Conclusions: After inhibiting *DNMT3B*, the expression of *GPX3* is upregulated, which may suppress the progression of OSCC.

Keywords: oral squamous cell carcinoma; methylation; DNA (cytosine-5-)-methyltransferase 3 beta; glutathione peroxidase 3; JNK/c-JUN signaling pathway

Introduction

The oral cavity is estimated to be the sixth most prevalent anatomical location affected by tumors, with approximately 275,000 new oral cancer cases reported globally [1]. Oral squamous cell carcinoma (OSCC) is the predominant histological subtype of oral cavity cancers, usually associated with a poor prognosis [2]. The standard treatment for OSCC involves the surgical resection of the tumor from the healthy tissue, and in advanced cases, the surgical removal of lymph nodes in the neck is also necessary. However, this approach can result in significant mutilation and a decreased quality of life for patients, highlighting the need for novel prognostic markers to better serve these patients [3,4].

DNA methylation, the covalent addition of methyl groups to the 5-carbon of cytosine rings, is a naturally occurring process in eukaryotic species. This epigenetic modification plays a pivotal role in several biological processes [5]. The enzyme DNA (cytosine-5-)-methyltransferase 3 beta (*DNMT3B*) is the major *de novo* DNA methyltransferase expressed during early embryonic development. It serves as the principal enzyme responsible for methylating the intragenic regions of actively transcribed genes [6]. Recent studies have further elucidated the implications of *DNMT3B* in DNA methylation, revealing its ability to modulate diverse biological functions, including those related to cancer [7,8]. *DNMT3B* and OCT4 expressions have been underlined to regulate the hepatocellular carcinoma cell resistance to sorafenib [9]. *DNMT3B* deficiency represses bladder cancer cells to migrate and invade by upregulating microRNA (miR)-34a [10]. The participations of DNA methylation and *DNMT3B* have also been evidenced in OSCC [11,12]. The objective of this research is to further evaluate the possible mechanisms implicated.

Journal of
BIOLOGICAL REGULATORS
and Homeostatic Agents

Table 1. Sequences used for transfection.

Gene	Sequence (5′-3′)
sh*DNMT3B* sense oligo	CCGGAGCTGTCCGAACTCGAAATAACTCGAGTTATTTCGAGTTCGGACAGCTTTTTTG
sh*DNMT3B* antisense oligo	AATTCAAAAAAGCTGTCCGAACTCGAAATAACTCGAGTTATTTCGAGTTCGGACAGCT
sh*GPX3* sense oligo	CCGGTGGAGGCTTTGTCCCTAATTTCTCGAGAAATTAGGGACAAAGCCTCCATTTTTG
sh*GPX3* antisense oligo	AATTCAAAAATGGAGGCTTTGTCCCTAATTTCTCGAGAAATTAGGGACAAAGCCTCCA
sh*NC* sense oligo	CCGCGAAATCGAGTTCGGACAGCTTTTTTGAGCGTCCGATGACTAACTCGAGTTATTT
sh*NC* antisense oligo	AATTCAAAATCGAAATAACTCGAGTTATTTCGAGTTCGGACAGCTAAGCTGCGAACTC

DNMT3B, DNA (cytosine-5-)-methyltransferase 3 beta; *GPX3*, glutathione peroxidase 3.

Besides random distribution across the genome, cytidine-phosphate-guanosine (CpG) dinucleotides are significantly underrepresented in mammalian genomes [13]. Most CpG dinucleotides are methylated, while some are clustered with lower methylation levels, referred to as CpG islands [14,15]. Among the genes known to be related to oral cancer, the database highlights glutathione peroxidase 3 (*GPX3*) as particularly noteworthy. This is suggested by the increase in *GPX3* expression following treatment with the DNA methyltransferase inhibitor 5-aza-2′-deoxycytidine (5-AzC), whose demethylation exerts a therapeutic impact on OSCC [16,17]. *GPX3* is a highly conserved protein that has been extensively studied and confirmed to act as a tumor suppressor in multiple cancer types, including OSCC [18,19]. Based on the predictions of bioinformatic tools, the promoter region of *GPX3* appears to contain CpG islands, suggesting the potential for methylation modifications of *GPX3*. Given the lack of reported evidence on the methylation modification of *DNMT3B* on *GPX3* in cancers, we initiated our research to confirm such modifications of *DNMT3B* on *GPX3* and to evaluate the interaction between *DNMT3B* and *GPX3* in OSCC, both of which are the major objectives of our study.

Materials and Methods

Bioinformatics

GPX3 expression was analyzed using the dataset GSE38823 from the Gene Expression Omnibus (GEO, https://www.ncbi.nlm.nih.gov/geo/) [16]. Data from The Cancer Genome Atlas (TCGA) (https://portal.gdc.cancer.gov/) were used to analyze the expressions of *DNMT3B* and *GPX3* in head and neck squamous cell carcinoma (HNSC). Additionally, the potential methylation modification on the *GPX3* promoter region was investigated using MethPrimer (https://www.urogene.org/methprimer/) [20].

Cell Culture

The human OSCC cell lines CAL27 (CBP60427, Cobioer, Nanjing, China) and HN-4 (BioVector NTCC, Beijing, China) were grown in Dulbecco's Modified Eagle's Medium (DMEM) (90113, Solabio Lifesciences, Beijing, China) supplemented with 10% fetal calf serum (FCS) (S9020, Solarbio Lifesciences, Beijing, China) and 1% antibiotics (P1400, Solarbio Lifesciences, Beijing, China). The human embryonic kidney cell line 293T (CBP64039, Cobioer, Nanjing, China) was maintained in the same conditions for lentivirus preparation. All cells were cultured in an incubator at 37 °C and 5% CO_2. They were routinely tested for short tandem repeat (STR) identification and mycoplasma contamination, and confirmed to be mycoplasma-free.

Lentivirus Preparation and Infection

The cDNA reference sequences of *DNMT3B* (NM_006892.4) and *GPX3* (NM_002084.5) were obtained from the National Center for Biotechnology Information (NCBI, Bethesda, MD, USA). The sequences of *DNMT3B* and *GPX3* short hairpin RNAs (shRNAs), and the control shRNA (shNC), which were available in Table 1, were inserted into the lentiviral backbone vector pFH-L (Hollybio, Shanghai, China). Meanwhile, *DNMT3B* and *GPX3* cDNAs were amplified, and the polymerase chain reaction (PCR) fragments were cloned into another lentivirus vector pGC-FU-3FLAG-IRES-Puromycin (GeneChem, Shanghai, China).

The vectors were then transfected into 293T cells using Lipofectamine™ 2000 transfection reagent (11668-500, Invitrogen, Carlsbad, CA, USA) along with the helper constructs. For the lentivirus infection, CAL27 and HN-4 cells were seeded in a 6-well plate (5×10^5 cells/well) and infected with the lentivirus at a multiplicity of infection (MOI) of 15 PFU/cell and the overexpression lentivirus at an MOI of 30 PFU/cell for 48 h before the assessments [21,22].

DNA Extraction and Quantitative Methylation-Specific PCR (qMSP) Analysis

These assays were performed in line with a previous study [23]. Following DNA extraction using the DNeasy Blood & Tissue kit (69504, Qiagen, Hilden, Germany), the genomic DNA underwent bisulfite modification with the Epitect Bisulfite kit (59104, Qiagen, Hilden, Germany). The modified DNA amplification was achieved using the AmpliTaq Gold Fast PCR kit (4390937, Applied Biosystems, Carlsbad, CA, USA) and the LightCycler 2.0 (Roche Diagnostics, Mannheim, Germany) was used to perform PCR amplification with the methylated (M) and unmethy-

lated (U) promoter sequences of *GPX3* under the following conditions: 95 °C for 10 min, followed by 35 cycles of 96 °C for 3 s, 59 °C for 3 s, 68 °C for 15 s, and 72 °C for 10 s.

The amplified products were analyzed using 1% agarose gel electrophoresis. The primers (5′-3′) used were: *GPX3*-methylated forward, TTGTTTTGGTTGTAATGGAGATC; reverse, TAAAAATCAAATCCCTATAAACGTA; *GPX3*-unmethylated forward, AAGAGAAGTCGAAGATGGAC; reverse, GGAGTTCTTTAGGAAAGTGTAG.

Chromatin Immunoprecipitation-PCR (ChIP-PCR) Assay

The Pierce™ Agarose ChIP kit (26156, ThermoFisher Scientific, Waltham, MA, USA) was used for this assay, following the manufacturer's protocol [24]. Specifically, the OSCC cell lines CAL-27 and HN-4 were cross-linked using 1% formaldehyde (F111939, Aladdin, Shanghai, China), and micrococcal nuclease (N128635, Aladdin, Shanghai, China) was employed to shear the chromatin in a water bath at 37 °C. Following the termination of the reaction, the harvested chromatin sample was incubated overnight at 4 °C with the primary antibodies against *DNMT3B* (ab227883, Abcam, Cambridge, UK) and *GPX3* (ab275965, Abcam, Cambridge, UK), along with 20 µL of protein A/G agarose. An antibody against IgG was used as a control. Following the elution of immunoprecipitation and DNA recovery, the purified DNA was subjected to the PCR analysis. The promoter sequences of *GPX3* used for this assay (5′-3′) were: forward, TGTCTCCCCTAAAGAAATAG; reverse, CTAGTGACCCTCAAAATAGG.

Transwell® Assay

Cell migration and invasion assays were performed using Transwell® chambers (8-µm pore; 3422, Corning, Inc., Corning, NY, USA) coated with Matrigel (for invasion test) (M8371, Solarbio Lifesciences, Beijing, China) or not (for migration test).

For the migration assay, 1×10^5 OSCC cells were maintained in serum-deprived medium in the upper Transwell® chamber, while the lower chamber contained complete medium with 10% FCS. After incubation for 48 h, cells in the upper chamber were removed with a cotton swab, and those in the lower chamber were fixed with 4% paraformaldehyde (P0099, Beyotime, Shanghai, China) at 4 °C for 20 min. Subsequently, cells were stained with 0.1% crystal violet (C8470, Solarbio Lifesciences, Beijing, China) at 25 °C for 30 min and observed under a light microscope (DP27, Olympus, Tokyo, Japan) at a total magnification of ×250. Cells in five randomly selected fields were counted and averaged. For the invasion assay, similar procedures were conducted, except that the upper chamber was additionally coated with Matrigel [25].

Table 2. Primer sequences used for qRT-PCR.

Gene	Sequence (5′-3′)
DNMT3B	
Forward	AGTGGTTAATAAGTCGAAGG
Reverse	ACACAGTGCAGTAAGACTGA
GPX3	
Forward	AAGAGAAGTCGAAGATGGAC
Reverse	GGAGTTCTTTAGGAAAGTGTAG
GAPDH	
Forward	CCTCAACTACATGGTTTACA
Reverse	TGTTGTCATACTTCTCATGG

qRT-PCR, quantitative real-time polymerase chain reaction; *GAPDH*, glyceraldehyde-3-phosphate dehydrogenase.

Flow Cytometry Assay

The OSCC cells designated for the apoptosis test were dissociated using EDTA-deprived trypsin (T1350, Solarbio Lifesciences, Beijing, China) and subsequently centrifuged at 300 ×*g* for 5 min at 4 °C. After washing, the cells were centrifuged under the same conditions and adjusted to a concentration of 1×10^5 cells. After resuspension in 1× binding buffer (100 µL), the cells were incubated with a mixture of 5 µL Annexin V-FITC and 10 µL PI staining solution provided with the kit (40302ES20, Yeason, Shanghai, China) for 15 min at room temperature in darkness. Finally, 1× binding buffer (400 µL) was added to the cells, and the results were analyzed using a CytoFLEX flow cytometer (Beckman Coulter, Indianapolis, IN, USA) along with its associated software.

Colony Formation Assay

Cell proliferation of OSCC was assessed using a colony formation assay. Specifically, OSCC cells (1×10^3) were plated in a 6-well plate for a 14-day culture period. Upon visible colony formation, the culture medium was discarded, followed by cell fixation using 4% paraformaldehyde and staining with 200 µL of crystal violet. Subsequently, the colonies were visualized and quantified using a digital camera (D500, Nikon, Tokyo, Japan).

Quantitative Real-Time PCR (qRT-PCR)

Total RNA was extracted from OSCC cells using a specific kit (DP419, TianGen, Beijing, China). The quantity and quality of the extracted RNA were assessed using a UV5 spectrophotometer (Mettler Toledo, Columbus, OH, USA). Complementary DNA (cDNA) was synthesized using a kit (KR103, TianGen, Beijing, China). Quantitative real-time PCR (qRT-PCR) was conducted using a 7500 Fast Real-Time PCR System (4351107, Applied Biosystems, Carlsbad, CA, USA) under the following thermocycling conditions: 94 °C for 3 min, 30 cycles of 94 °C for 30 s, 55 °C for 30 s and 72 °C for 1 min, and 72 °C for 5

Journal of
BIOLOGICAL REGULATORS
and Homeostatic Agents

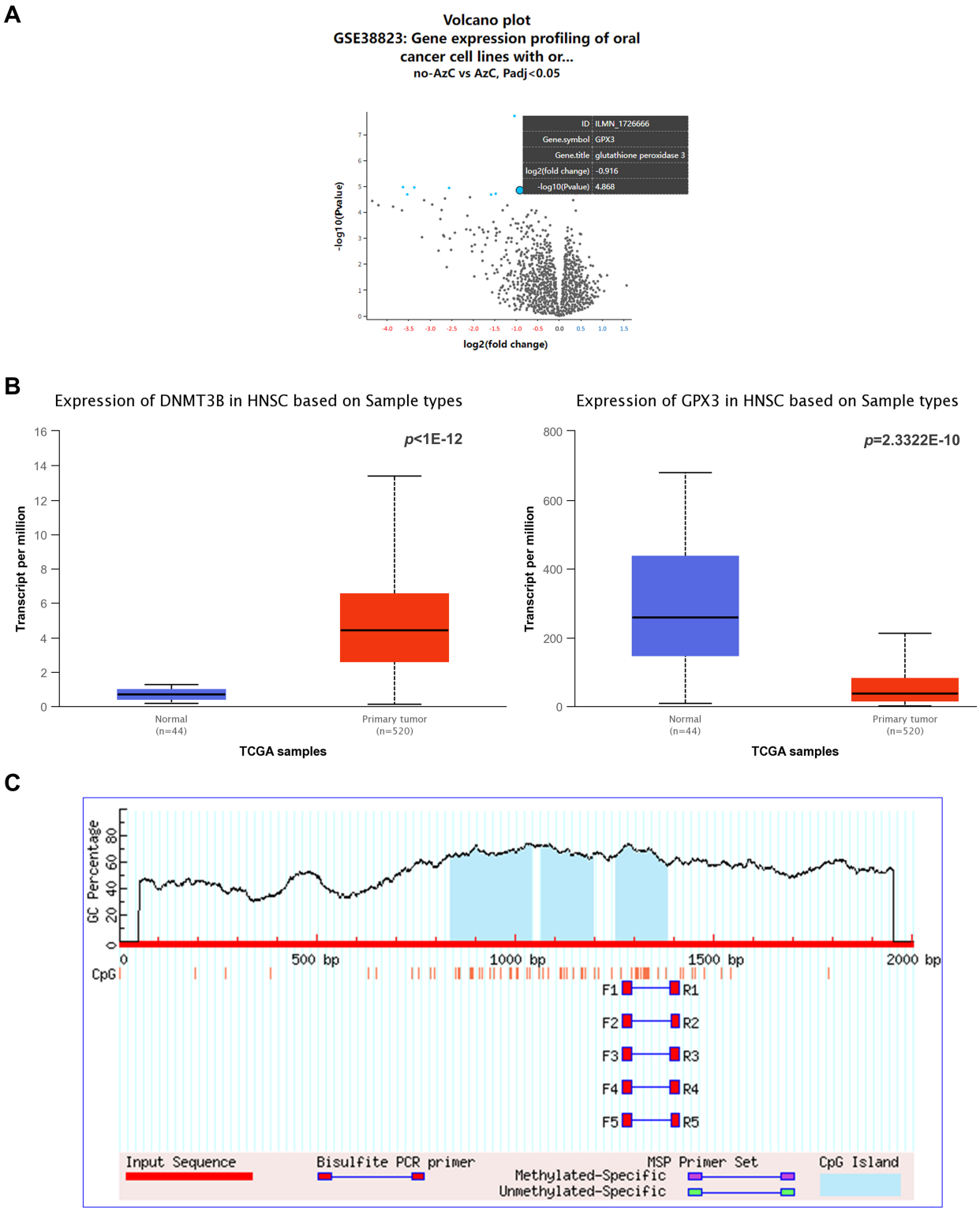

Fig. 1. Expression patterns of *DNMT3B* and *GPX3* in HNSC and the possible methylation of *GPX3*. (A) The expression pattern of *DNMT3B* is based on the dataset GSE38823 from GEO (https://www.ncbi.nlm.nih.gov/geo/). The red color of the horizontal axis indicates the gene expression with negative log2 (fold change), and the blue color indicates the gene expression with positive log2 (fold change). (B) The expression patterns of *DNMT3B* and *GPX3* are based on the data from the TCGA database (https://portal.gdc.cancer.gov/). (C) The existence of cytidine-phosphate-guanosine (CpG) islands within the promoter sequence of *GPX3* is confirmed by MethPrimer (https://www.urogene.org/methprimer/). Abbreviations: HNSC, head and neck squamous cell carcinoma; GEO, Gene Expression Omnibus; TCGA, The Cancer Genome Atlas.

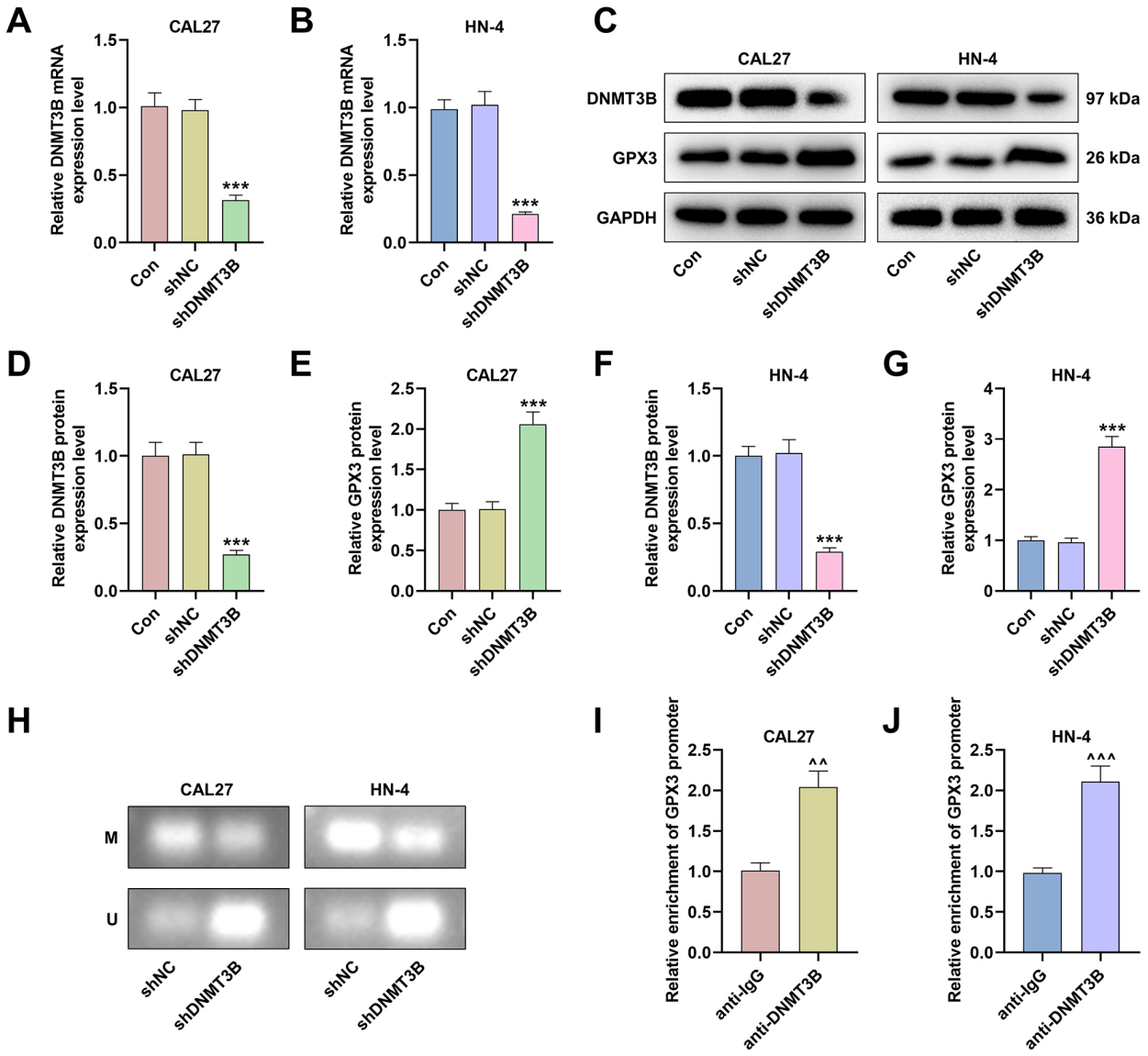

Fig. 2. Impact of sh*DNMT3B* upon the expression of both *DNMT3B* and *GPX3* and the possible methylation of *GPX3*. (A,B) Quantification of *DNMT3B* mRNA levels in OSCC cell lines (CAL27 and HN-4) following the silencing of *DNMT3B* through qRT-PCR (*GAPDH* as the housekeeping control). (C–G) The protein levels of DNMT3B and GPX3 in OSCC cell lines (CAL27 and HN-4) after the silencing of DNMT3B using Western blot. GAPDH was used as the internal control. (H) The methylation levels of the *GPX3* promoter (qMSP assay). (I,J) The binding between *DNMT3B* and *GPX3* promoters in OSCC cell lines (CAL27 and HN-4) using ChIP-PCR assay. All data from three independent tests were presented as mean ± SD. ***$p < 0.001$ *vs* shNC; $^{\wedge\wedge}p < 0.01$, $^{\wedge\wedge\wedge}p < 0.001$ *vs* anti-IgG. Abbreviations: Con, Control; shNC, short hairpin RNA negative control; sh*DNMT3B*, *DNMT3B*-specific short hairpin RNA; qMSP, quantitative methylation-specific PCR; ChIP-PCR, chromatin immunoprecipitation-PCR; GAPDH, glyceraldehyde-3-phosphate dehydrogenase; M, methylation; U, unmethylation; OSCC, oral squamous cell carcinoma.

min. The mRNA expression levels were quantified using the $2^{-\Delta\Delta Ct}$ method [26]. The primer sequences used in the qRT-PCR are provided in Table 2.

Western Blotting

Total protein was isolated using radioimmunoprecipitation assay (RIPA) lysis buffer (89901, ThermoFisher Scientific, Waltham, MA, USA) and its concentration was determined with the bicinchoninic acid (BCA) protein assay kit (23225, ThermoFisher Scientific, Waltham, MA, USA). The protein samples were separated by SDS-PAGE (P1200, Solarbio Lifescience, Beijing, China) and transferred onto a polyvinylidene difluoride (PVDF) membrane (YA1701, Solarbio Lifescience, Beijing, China). The membrane was then incubated with primary antibodies against DNMT3B (ab2851, 97 kDa, 1:2000, abcam, London, UK), GPX3 (ab275965, 26 kDa, 1:1000, abcam, London, UK), phosphorylated (p)-Jun N-terminal kinase (JNK, ab215208, 48

Journal of
BIOLOGICAL REGULATORS
and Homeostatic Agents

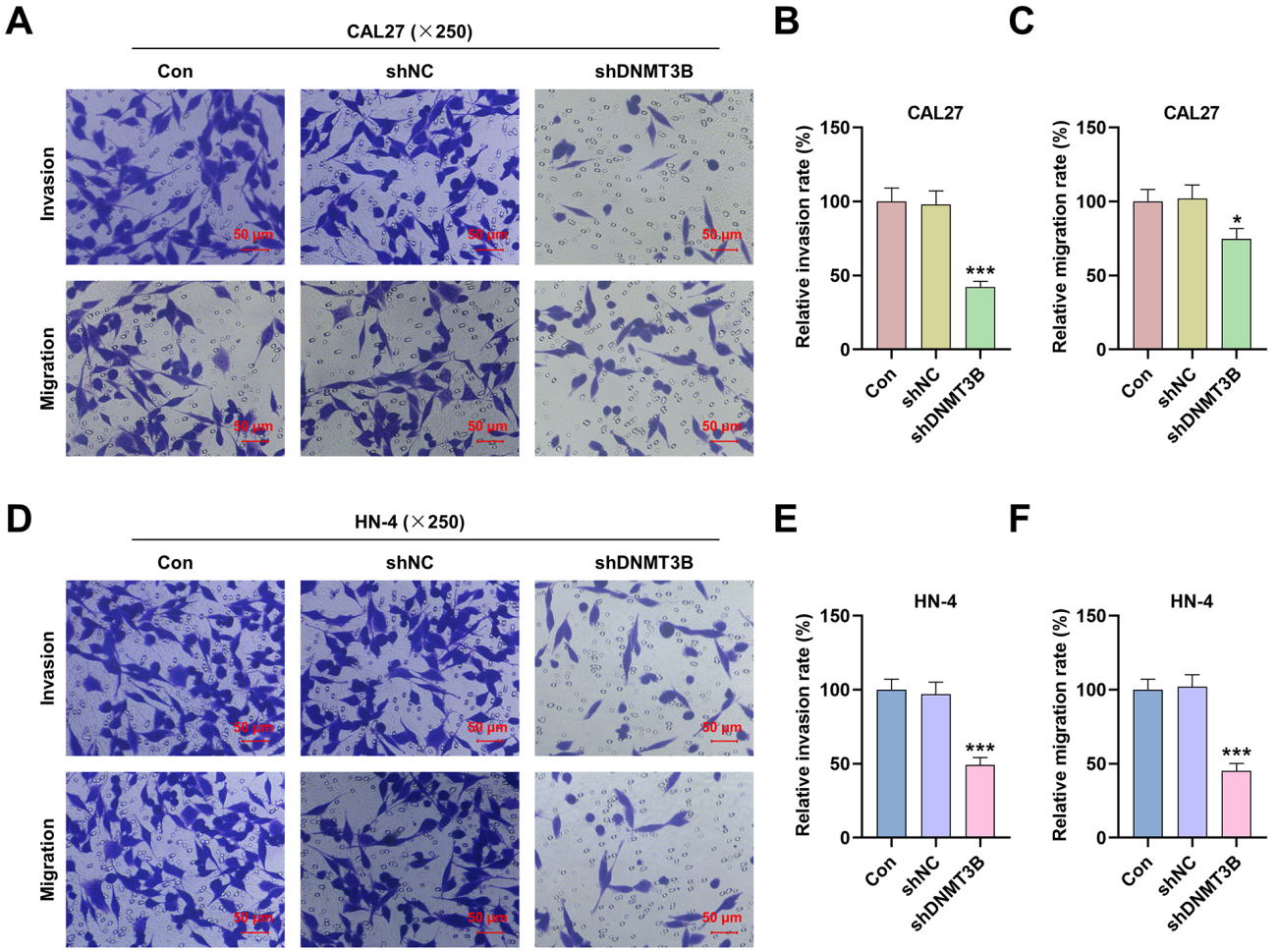

Fig. 3. Impact of shDMNT3B on OSCC cell invasion and migration. (A–F) The role of *DNMT3B* silencing in the invasion and migration of OSCC cell lines (CAL27 and HN-4) using Transwell® assay. Total magnification: ×250. Scale bar = 50 μm. All data from three independent tests were presented as mean ± SD. *$p < 0.05$, ***$p < 0.001$ *vs* shNC.

kDa, 1:1000, abcam, London, UK), JNK (ab110724, 48 kDa, 1:2000, abcam, London, UK), p-c-JUN (ab32385, 36 kDa, 1:2000, abcam, London, UK), c-JUN (ab32137, 36 kDa, 1:2000, abcam, London, UK), and the housekeeping control glyceraldehyde-3-phosphate dehydrogenase (GAPDH, ab8245, 36 kDa, 1:2000, abcam, London, UK) overnight at 4 °C. Subsequently, the membrane was incubated with horseradish peroxide (HRP)-conjugated secondary antibodies against rabbit IgG (SE134, 1:2000, Solarbio Lifesciences, Beijing, China) and mouse IgG (SE131, 1:2000, Solarbio Lifesciences, Beijing, China). After washing with TBST (28360, ThermoFisher Scientific, Waltham, MA, USA), the protein bands were visualized using an ECL visualization substrate (32106, ThermoFisher Scientific, Waltham, MA, USA). The Chemi-Doc Imaging system (Bio-Rad Laboratories, Hercules, CA, USA) and ImageJ (version 1.48, National Institutes of Health, Bethesda, MA, USA) were used to analyze the gray value data, with GAPDH serving as the loading control [27].

Statistical Analysis

The values of the three independent tests were expressed as the mean ± standard deviation (SD). Statistical analyses were performed using GraphPad 8 (GraphPad, Inc., La Jolla, CA, USA). Differences among or between groups were addressed using one-way analysis of variance (ANOVA) or independent samples *t*-test, with *post hoc* Bonferroni test. Statistical significance was defined as a *p*-value less than 0.05.

Results

Expression Patterns of DNMT3B and GPX3 in HNSC and the Possible Methylation Modification in the GPX3 Promoter

To further investigate the implications of *DNMT3B* and *GPX3* in OSCC and the possible role of *GPX3* in *DNMT3B*-mediated methylation, the expression patterns of these genes were analyzed based on the dataset GSE38823 from GEO (Fig. 1A) and TCGA (Fig. 1B,C). The anal-

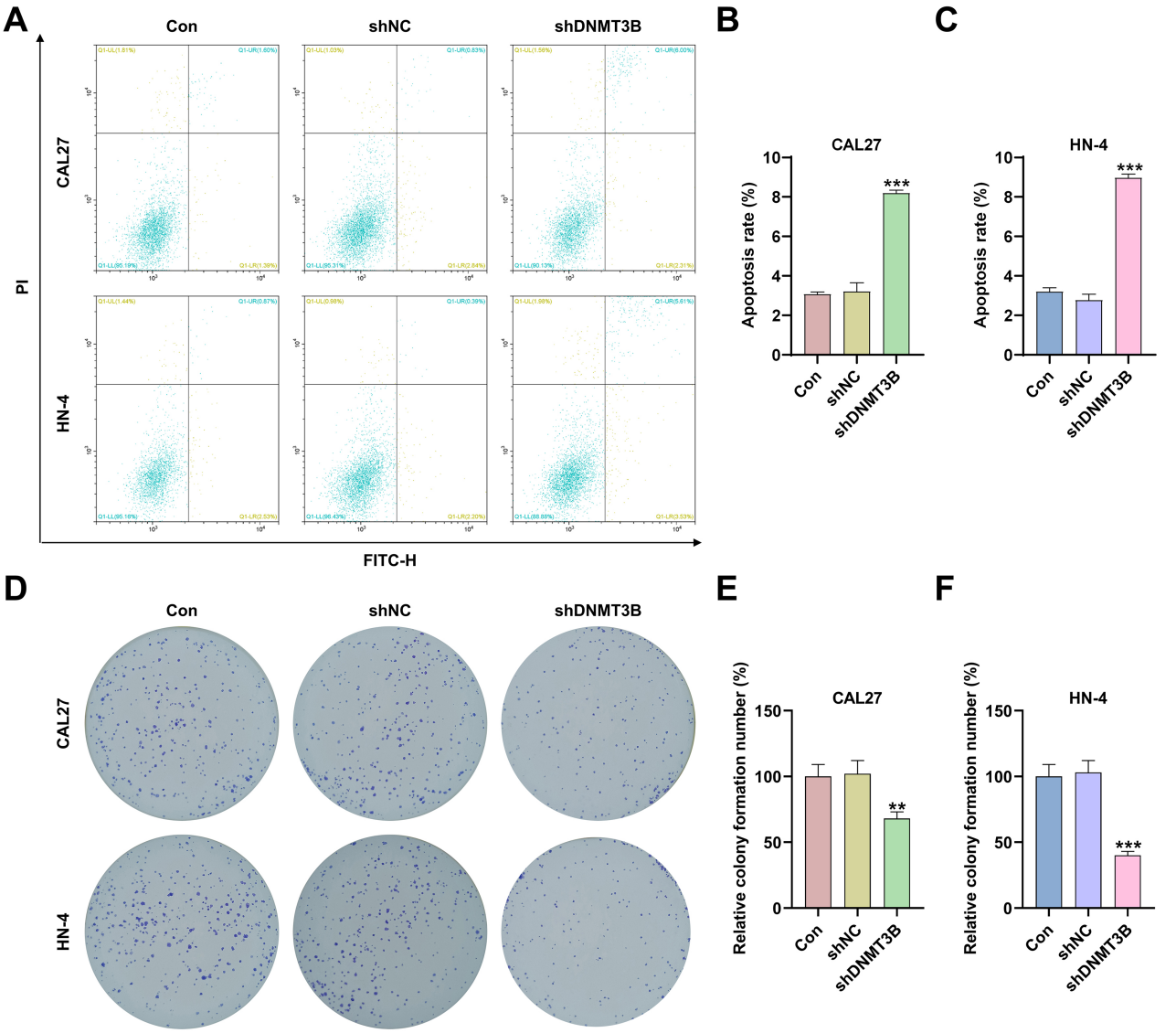

Fig. 4. Impact of sh*DNMT3B* on OSCC cell apoptosis and proliferation. (A–C) The influence of *DNMT3B* silencing on the apoptosis of OSCC cell lines (CAL27 and HN-4) using flow cytometry. (D–F) The influence of *DNMT3B* silencing on the proliferation of OSCC cell lines (CAL27 and HN-4) using colony formation assay. All data from three independent tests were presented as mean ± SD. $^{**}p < 0.01$, $^{***}p < 0.001$ *vs* shNC.

ysis revealed that the expression level of *GPX3* was elevated following treatment with the DNA methylation inhibitor 5-AzC (Fig. 1A). Additionally, the analysis showed that *DNMT3B* expression was significantly higher ($p < 1 \times 10^{-12}$) (Fig. 1B) in HNSC samples (n = 520) compared to normal samples (n = 44). Conversely, *GPX3* expression was significantly lower ($p = 2.3322 \times 10^{-10}$) (Fig. 1B) in HNSC samples compared to normal samples. Further investigation using the MethPrimer tool confirmed the presence of CpG islands within the promoter sequence of the *GPX3* gene (Fig. 1C), revealing the possible methylation modification of *GPX3*.

Impacts of shDNMT3B upon the Expressions of both DNMT3B and GPX3 and the Methylation of GPX3 in OSCC Cells

We subsequently analyzed the expression levels of *DNMT3B* and *GPX3* in OSCC cell lines CAL27 and HN-4 following the silencing of *DNMT3B*. We also measured the methylation level of the *GPX3* gene. The results showed that silencing *DNMT3B* (sh*DNMT3B*) significantly repressed the expression of *DNMT3B* but promoted the expression of *GPX3* ($p < 0.001$) (Fig. 2A–G). Furthermore, the qMSP and ChIP-PCR assay results suggested that depletion of *DNMT3B* could substantially reduce the methylation of the *GPX3* promoter (Fig. 2H). Additionally, the ChIP-PCR data indicated that *DNMT3B* could directly bind to the promoter region of *GPX3* ($p < 0.01$) (Fig. 2I,J).

Journal of
BIOLOGICAL REGULATORS
and Homeostatic Agents

Impact of shDMNT3B on the Invasion, Migration, Apoptosis, and Proliferation of OSCC Cells

The impact of *DNMT3B* silencing on OSCC cell invasion and migration was evaluated using the Transwell® assay. The results showed that the capacities of CAL27 and HN-4 cells to invade and migrate were significantly diminished after silencing *DNMT3B* ($p < 0.05$) (Fig. 3A–F).

Using flow cytometry (Fig. 4A–C) and colony formation assays (Fig. 4D–F), we further confirmed that the depletion of *DNMT3B* could accelerate the apoptosis and restrain the proliferation of OSCC cells CAL27 and HN-4 ($p < 0.01$) (Fig. 4A–F).

Impact of shDNMT3B on the JNK Signaling Pathway in OSCC Cells

The involvement of the JNK signaling pathway in OSCC has been evidenced [28]. Therefore, we hypothesized that the JNK pathway may be implicated in the mechanism by which sh*DNMT3B* influenced OSCC and that the levels of JNK signaling pathway-related factors would be diminished in the OSCC cell lines CAL27 and HN-4 following the depletion of *DNMT3B*. It was observed that the phosphorylation levels of JNK and c-JUN in these cells were significantly decreased after silencing *DNMT3B* ($p < 0.01$) (Fig. 5A–E).

Impacts of GPX3 on the Invasion, Migration, Apoptosis, and Proliferation of OSCC Cells

Here, we explored the impact of *GPX3* on OSCC. We successfully transfected overexpression and silencing vectors of *GPX3* into OSCC cell lines CAL27 and HN-4 ($p < 0.001$) (Fig. 6A,B). Subsequently, we investigated how *GPX3* influences OSCC cell invasion and migration using Transwell® assay. The results showed that overexpression of *GPX3* could block OSCC cell invasion and migration, while *GPX3* deficiency had the opposite effect ($p < 0.001$) (Fig. 6C–H).

The apoptosis rate of OSCC cells was significantly increased following the overexpression of *GPX3*. Conversely, silencing *GPX3* had the opposite effect ($p < 0.01$) (Fig. 7A–C). Additionally, the colony formation assay results indicated that overexpression of *GPX3* reduced while *GPX3* silencing increased the number of colonies formed in both OSCC cell lines ($p < 0.001$) (Fig. 7D–F).

Impact of GPX3 on the JNK Signaling Pathway in OSCC Cells

The roles of GPX3 in the JNK signaling pathway were investigated using Western blot analysis. The results revealed that the overexpression of GPX3 inhibited the phosphorylation of JNK and c-JUN in both OSCC cell lines. Conversely, silencing GPX3 led to contrasting effects on the phosphorylation of JNK and c-JUN in the same OSCC cell lines ($p < 0.05$) (Fig. 8A–E).

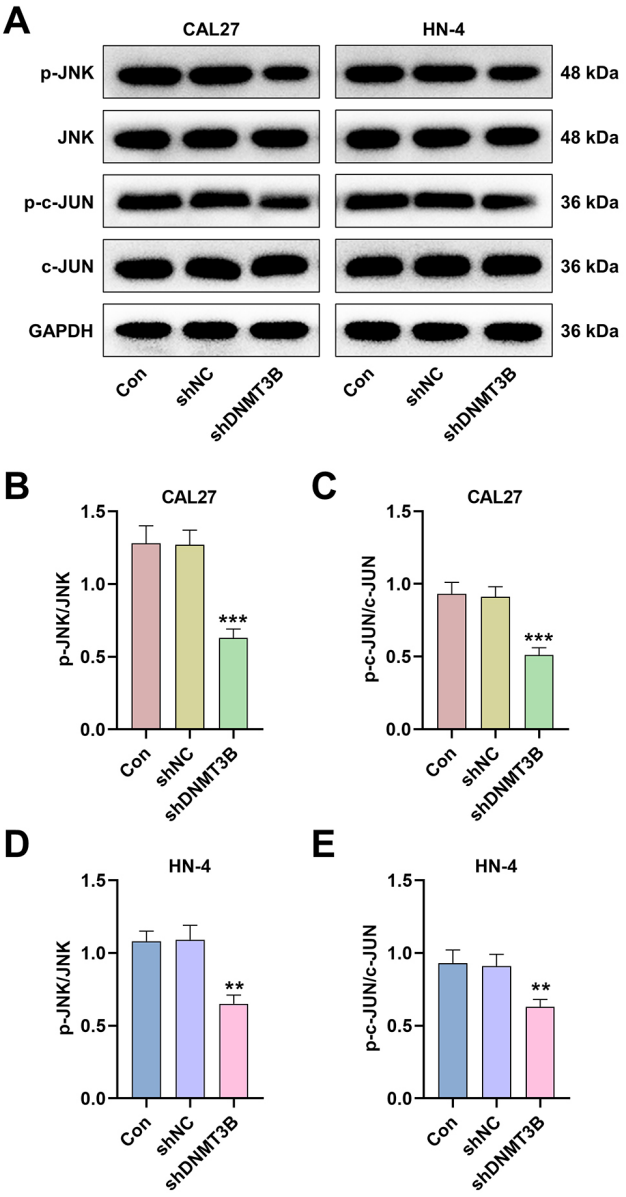

Fig. 5. Impact of sh*DNMT3B* on the Jun N-terminal kinase (JNK)/c-JUN signaling pathway in OSCC cells. (A–E) Effect of *DNMT3B* silencing on JNK/c-JUN signaling pathway-related factors (p-JNK, JNK, p-c-JUN and c-JUN) in OSCC cell lines (CAL27 and HN-4) using Western blot. GAPDH was employed as the housekeeping gene. All data from three independent tests were presented as mean ± SD. $^{**}p < 0.01$, $^{***}p < 0.001$ *vs* shNC.

Reversing the Effects of shDNMT3B on the Invasion, Migration, Apoptosis, and Proliferation of OSCC Cells through shGPX3

This study investigates the interaction between *DNMT3B* and *GPX3* in OSCC cells. The findings revealed that the effects of *DNMT3B* silencing on OSCC cell invasion and migration were reversed by silencing *GPX3* ($p < 0.01$) (Fig. 9A–F). Additionally, the results of flow cytometry and colony formation assays suggested that the silencing of *GPX3* attenuated the effects of *DNMT3B* silencing

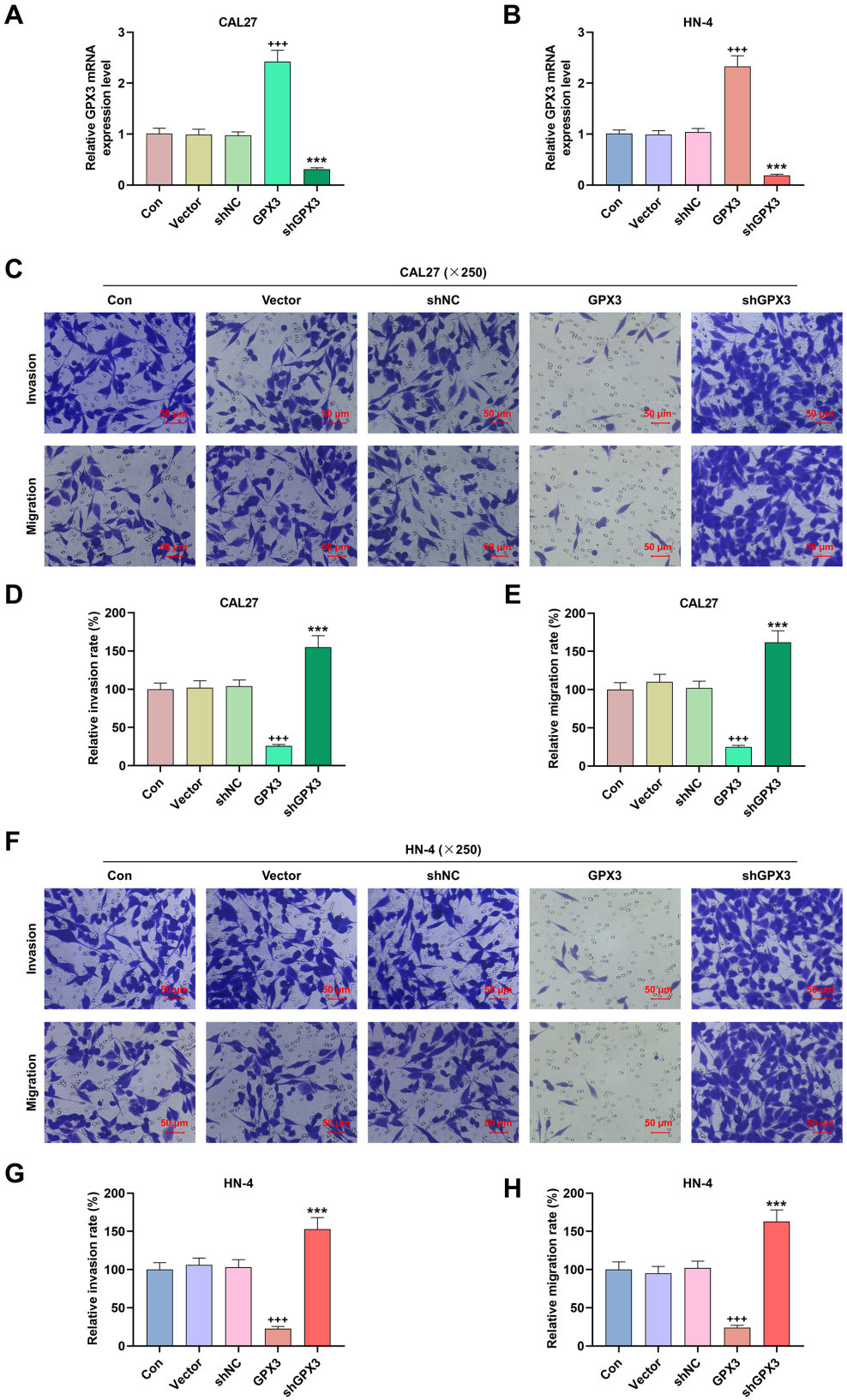

Fig. 6. Impact of *GPX3* on OSCC cell invasion and migration. (A,B) *GPX3* mRNA levels in OSCC cell lines (CAL27 and HN-4) following the overexpression and silencing of *GPX3* using quantitative reverse-transcription PCR. GAPDH was used as the housekeeping control. (C–H) The roles of *GPX3* overexpression and silencing in the invasion and migration of OSCC cell lines (CAL27 and HN-4) employing Transwell® assay. Total magnification: ×250. Scale bar = 50 μm. All data from three independent tests were presented as mean ± SD. $^{+++}p < 0.001$ *vs* Vector; $^{***}p < 0.001$ *vs* shNC.

Journal of
BIOLOGICAL REGULATORS
and Homeostatic Agents

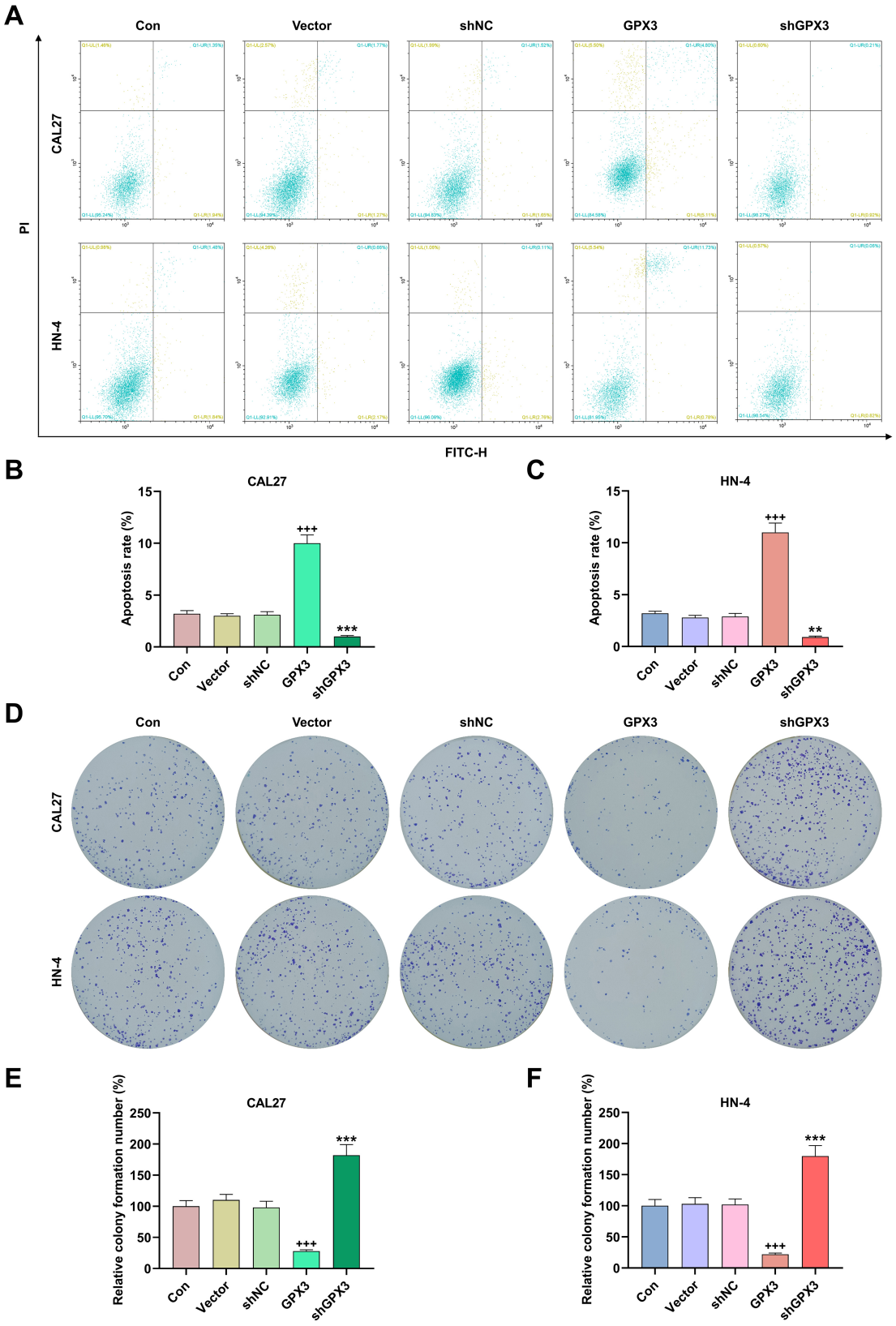

Fig. 7. Impact of *GPX3* on OSCC cells apoptosis and proliferation. (A–C) The roles of *GPX3* overexpression and silencing in OSCC cell apoptosis (CAL27 and HN-4) by flow cytometry. (D–F) The impact of *GPX3* overexpression and silencing on OSCC cells (CAL27 and HN-4) proliferation through colony formation assay. All data from three independent tests were presented as mean ± SD. $^{+++}p < 0.001$ *vs* Vector; $^{**}p < 0.01$, $^{***}p < 0.001$ *vs* shNC.

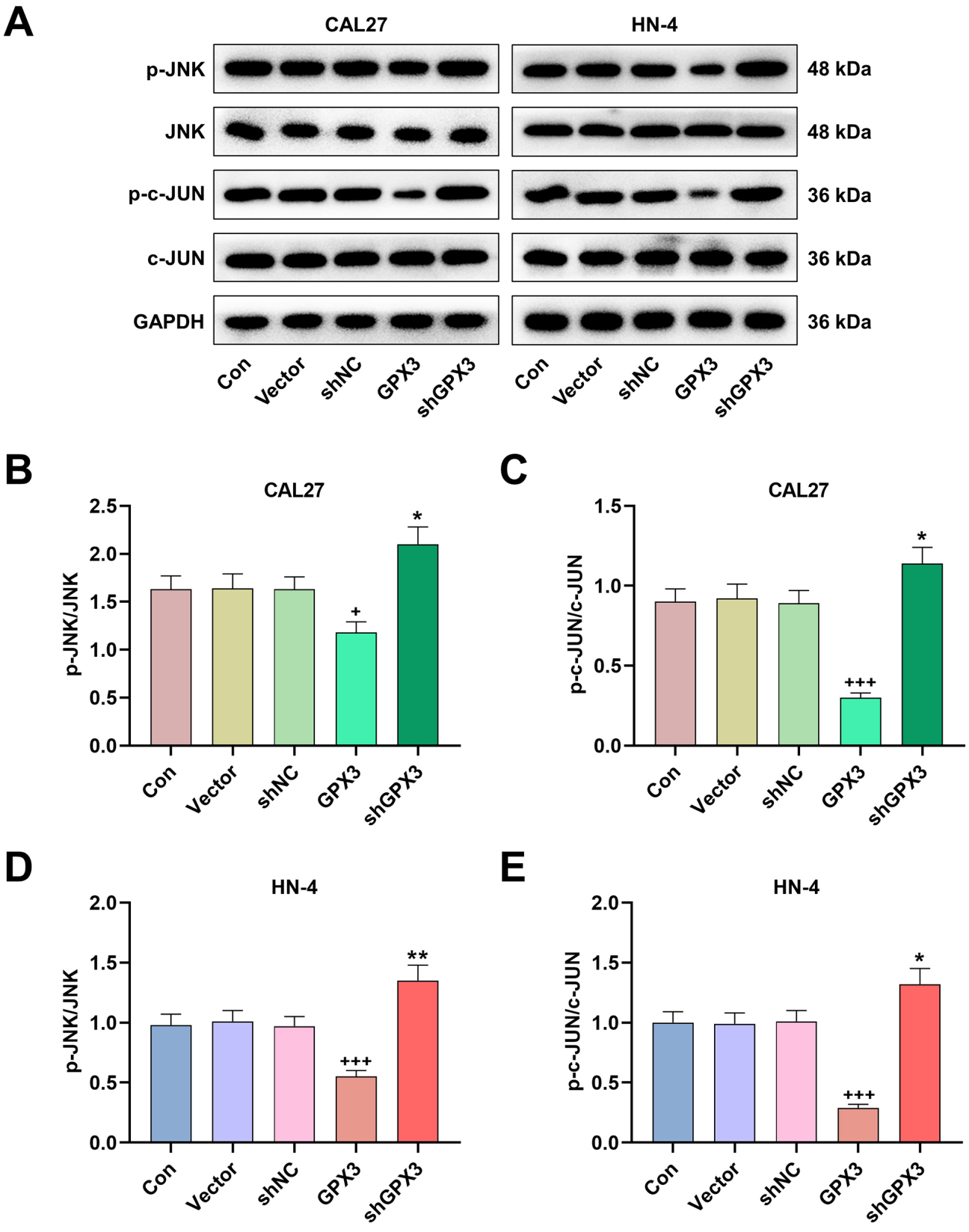

Fig. 8. Influence of GPX3 on the JNK/c-JUN signaling pathway in OSCC cells. (A–E) The effects of overexpression and silencing of GPX3 in JNK/c-JUN signaling pathway-related factors (p-JNK, JNK, p-c-JUN, and c-JUN) in OSCC cell lines (CAL27 and HN-4) using Western blot, with GAPDH serving as the loading control. All data of three independent tests were presented as mean ± SD. $^{+}p < 0.05$, $^{+++}p < 0.001$ *vs* Vector; $*p < 0.05$, $**p < 0.01$ *vs* shNC.

Journal of
BIOLOGICAL REGULATORS
and Homeostatic Agents

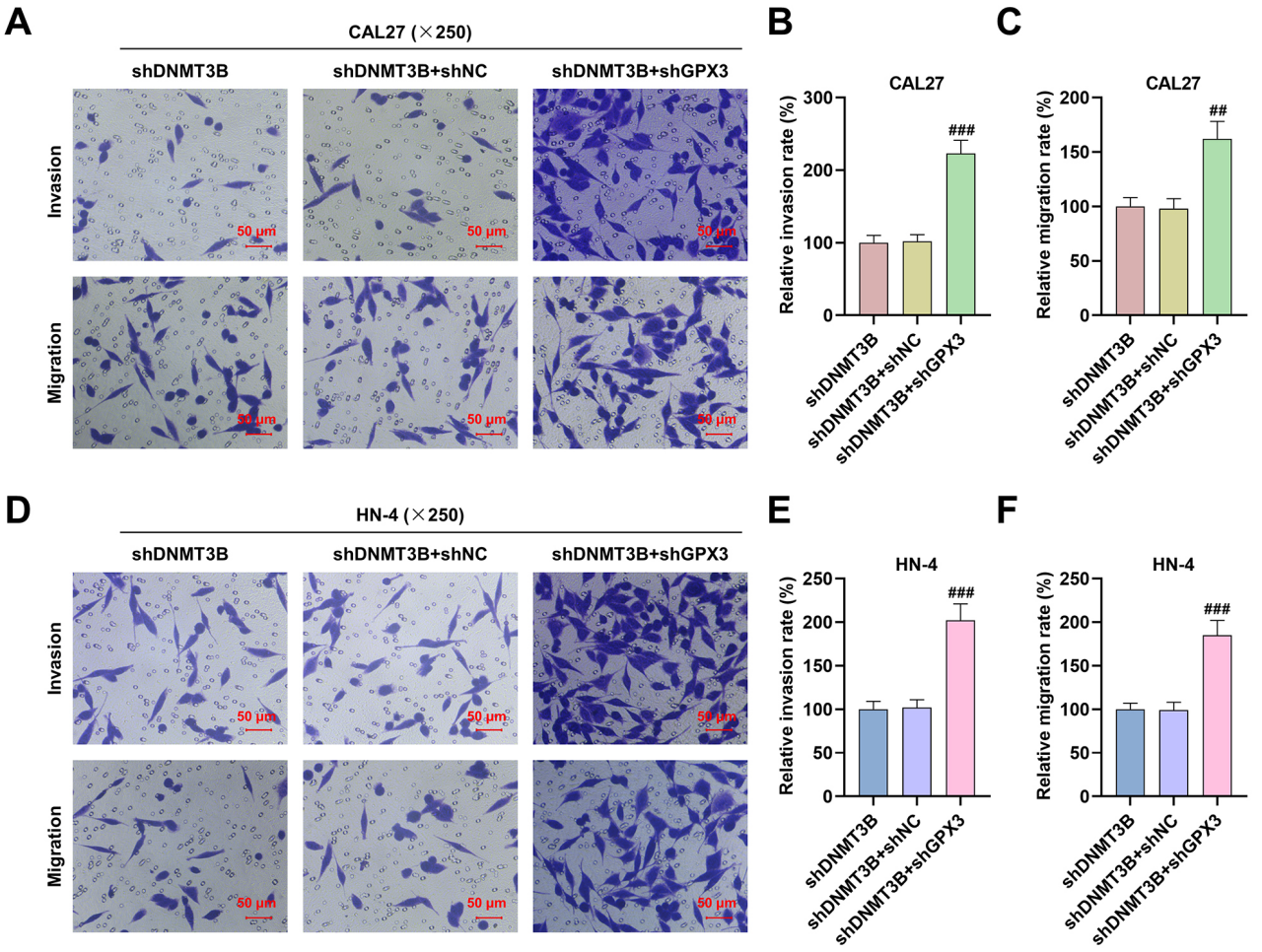

Fig. 9. Reversing the effects of sh*DNMT3B* on the invasion and migration of OSCC cells through sh*GPX3*. (A–F) The effects of both *DNMT3B* and *GPX3* silencing on OSCC cell (CAL27 and HN-4) invasion and migration using Transwell® assay. Total magnification: ×250. Scale bar = 50 μm. All data of three independent tests were presented as mean ± SD. $^{\#\#}p < 0.01$, $^{\#\#\#}p < 0.001$ *vs* sh*DNMT3B*+shNC.

on both apoptosis and proliferation of OSCC cells ($p < 0.01$) (Fig. 10A–F). Furthermore, the study demonstrated that the impacts of *DNMT3B* silencing on the protein expressions of GPX3 and JNK signaling pathway-related factors (phosphorylated JNK and c-JUN) were reversed by silencing *GPX3* ($p < 0.001$) (Fig. 11A–G).

Discussion

Previous research has examined the potential implications and effects of *DNMT3B* and *GPX3* in OSCC. These studies have suggested a tumor-promotive effect for *DNMT3B* and a tumor-repressive function for *GPX3* in OSCC [12,19]. In this work, we aimed to further investigate the link between these two genes in OSCC. Based on bioinformatics analyses, we found that *DNMT3B* expression was elevated, while *GPX3* expression was reduced, in HNSC. Additionally, the promoter region of *GPX3* contains CpG islands, suggesting potential epigenetic regulation. Our results confirm that silencing *DNMT3B* can demethylate the *GPX3* promoter, leading to the repression of OSCC cell proliferation, migration, and invasion, while promoting apoptosis in CAL27 and HN-4 cell lines through mediating JNK signaling pathway. These findings provide further evidence for the *DNMT3B*-mediated DNA methylation and the interaction between *DNMT3B* and *GPX3* in OSCC.

De novo DNMT3B-mediated DNA methylation at cytosines is crucial for genome regulation and development, with its dysfunction implicated in various diseases, including cancer [29]. In addition to the documented biological effects of *DNMT3B* on tumor cell proliferation, migration, and invasion, the overexpression of *DNMT3B* can lead to a hypermethylator phenotype in human cancer cells like breast cancer [30,31]. This overexpression also plays a significant role and holds predictive value in the prognosis of oral cancer [30–32]. Building on previous findings regarding *DNMT3B*'s potential role in different cancers, including oral cancer, where DMNT3B silencing represses the migration and invasion of bladder cancer cells [10,12,33], we additionally confirmed that *DNMT3B* was higher-expressed

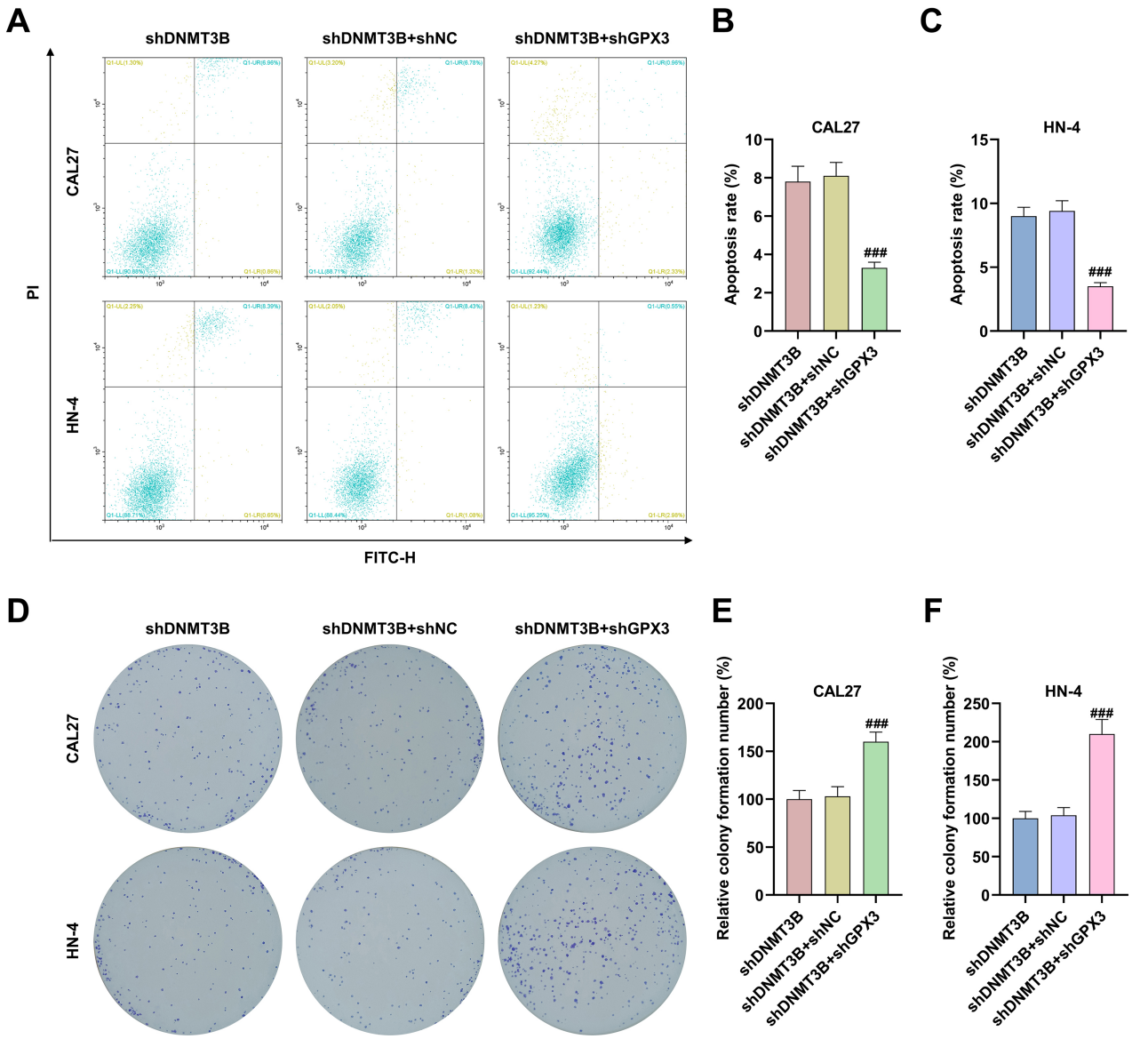

Fig. 10. Reversing the impact of sh*DNMT3B* on the apoptosis and proliferation of OSCC cells by sh*GPX3*. (A–C) The roles of both *DNMT3B* and *GPX3* silencing in the apoptosis of OSCC cell lines (CAL27 and HN-4) by flow cytometry assay. (D–F) The roles of both *DNMT3B* and *GPX3* silencing in the proliferation of OSCC cell lines (CAL27 and HN-4) by colony formation assay. All data of three independent tests were presented as mean ± SD. $^{###}p < 0.001$ *vs* sh*DNMT3B*+shNC.

in HNSC, and *DNMT3B* silencing blocked the proliferation, migration and invasion yet promoted the apoptosis of OSCC cells CAL27 and HN-4. Moreover, it is important to highlight that the genomes of vertebrates exhibit high methylation levels at cytosine residues within CpG sequences. This CpG methylation plays a pivotal role in silencing epigenetic genes, ensuring genome stability. Notably, the expression of *GPX3* increased significantly after treatment with 5-AzC, the demethylation of which exerts a therapeutic effect on OSCC [16,17,34]. Furthermore, MethPrimer predictions confirmed the presence of CpG island (CpG-rich region in the promoter) in the *GPX3* promoter region [20,35]. This suggests that *GPX3* may be a downstream target of *DNMT3B*, implicating its involvement in the mechanisms through which *DNMT3B* influences OSCC. *GPX3*, an extracellular glutathione, plays dual roles in tumors, with its promoter methylation linked to various biological effects [36,37]. Moreover, *GPX3* has regulatory effects on malignant cell migration, invasion, and chondrocyte apoptosis [38,39]. This study shows decreased *GPX3* levels in HNSC, and silencing *DNMT3B* significantly reduces *GPX3* methylation and increases *GPX3* levels in OSCC cells. Notably, *DNMT3B* silencing effects on OSCC cells were reversed following *GPX3* silencing, proving the interaction between *DNMT3B* and *GPX3* and the involvement of *DNMT3B*-mediated *GPX3* methylation in OSCC.

Journal of
BIOLOGICAL REGULATORS
and Homeostatic Agents

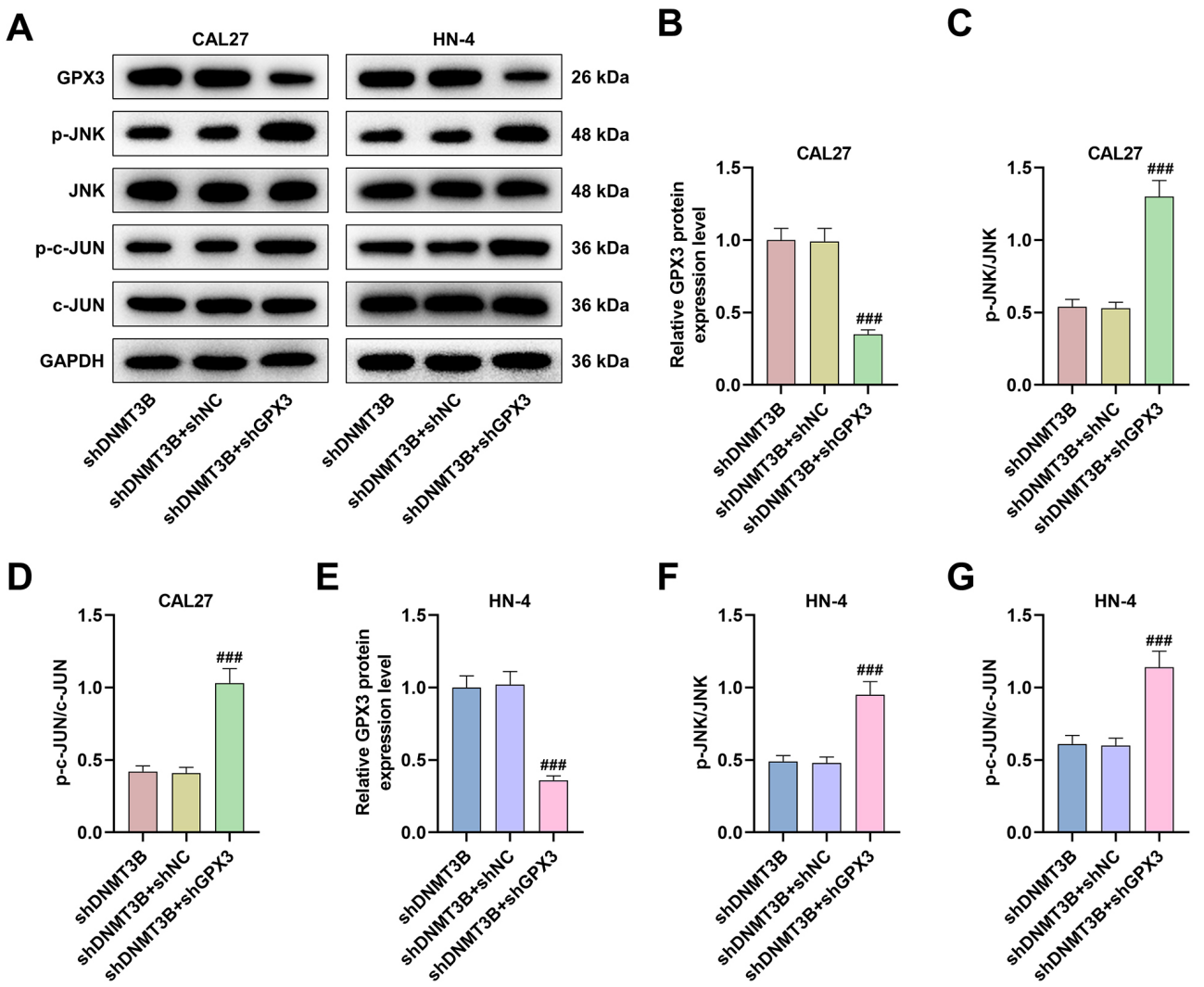

Fig. 11. Reversing the effects of shDNMT3B on the GPX3/JNK signaling pathway in OSCC cells through shGPX3. (A–G) The effects of both DNMT3B and GPX3 silencing on GPX3, p-JNK, JNK, p-c-JUN, and c-JUN protein levels in OSCC cell lines (CAL27 and HN-4) using Western blot, with GAPDH as the housekeeping gene. All data of three independent tests were delineated as mean ± SD. $^{###}p < 0.001$ *vs* shDNMT3B+shNC.

Upon investigating the potential mechanism implicated, the JNK signaling pathway captured our attention. This interest is supported by findings from different studies that have linked DNA methylation, *GPX3*, and the JNK pathway [38,40]. JNKs belong to the evolutionarily conserved subgroup of mitogen-activated protein kinases (MAPKs), and recent insights have revealed their role in regulating various physiological processes such as proliferation, survival, differentiation, and apoptosis [41,42]. Furthermore, the promotive effects of both JNK and its downstream signaling molecule c-JUN have been well-documented in cancer research [43]. By combining the roles of *DNMT3B*-mediated methylation, *GPX3*, and the JNK signaling pathway in OSCC, it was observed that the silence of *DNMT3B* led to the suppression of both JNK and c-JUN phosphorylation, which was contrary to the effects of *GPX3* silencing. Furthermore, *GPX3* silencing attenuated the influence of *DNMT3B* knockdown on the phosphorylation of JNK and c-JUN in OSCC cells, from which we concluded that the effects of *DNMT3B* silencing on OSCC cells were achieved via regulating the *GPX3*/JNK signaling axis. Our future research will use pathway antagonists or agonists to verify the regulatory effect of *DNMT3B* and *GPX3* in the JNK/c-JUN pathway. In addition, we plan to employ methylase following *DNMT3B* knockdown to prove that *DNMT3B* could potentially regulate the progression of OSCC by influencing the methylation of the *GPX3* promoter.

Conclusions

By linking *DNMT3B*-mediated DNA methylation with *GPX3* and the JNK pathway, our study demonstrates that silencing *DNMT3B* promotes *GPX3* level to inhibit the

proliferation, migration, and invasion but induce the apoptosis of OSCC cells, which may be related to the inactivation of the JNK/c-JUN signaling pathway.

Availability of Data and Materials

The analyzed data sets generated during the study are available from the corresponding author on reasonable request.

Author Contributions

Substantial contributions to conception and design: RFZ. Data acquisition, data analysis and interpretation: XZX, YTM, YYL, JWZ. Drafting the article or critically revising it for important intellectual content: All authors. Final approval of the version to be published: All authors. Agreement to be accountable for all aspects of the work in ensuring that questions related to the accuracy or integrity of the work are appropriately investigated and resolved: All authors.

Ethics Approval and Consent to Participate

Not applicable.

Acknowledgment

Not applicable.

Funding

This work was supported by the Jiangsu Graduate Students' innovation and entrepreneurship training program [SJCX23_1390].

Conflict of Interest

The authors declare no conflict of interest.

References

[1] Melo BADC, Vilar LG, Oliveira NRD, Lima POD, Pinheiro MDB, Domingueti CP, *et al*. Human papillomavirus infection and oral squamous cell carcinoma - a systematic review. Brazilian Journal of Otorhinolaryngology. 2021; 87: 346–352.

[2] Ramos JC, Dos Santos ES, Normando AGC, Alves FA, Kowalski LP, Santos-Silva AR, *et al*. Oral squamous cell carcinoma around dental implants: a systematic review. Oral Surgery, Oral Medicine, Oral Pathology and Oral Radiology. 2021; 131: 660–674.

[3] Olek M, Machorowska-Pieniążek A, Olek K, Cieślar G, Kawczyk-Krupka A. Photodynamic therapy in the treatment of oral squamous cell carcinoma - The state of the art in preclinical research on the animal model. Photodiagnosis and Photodynamic Therapy. 2021; 34: 102236.

[4] Mascitti M, Togni L, Caponio VCA, Zhurakivska K, Bizzoca ME, Contaldo M, *et al*. Lymphovascular invasion as a prognostic tool for oral squamous cell carcinoma: a comprehensive review. International Journal of Oral and Maxillofacial Surgery. 2022; 51: 1–9.

[5] Li S, Tollefsbol TO. DNA methylation methods: Global DNA methylation and methylomic analyses. Methods. 2021; 187: 28–43.

[6] Gagliardi M, Strazzullo M, Matarazzo MR. DNMT3B Functions: Novel Insights From Human Disease. Frontiers in Cell and Developmental Biology. 2018; 6: 140.

[7] Zhang J, Yang C, Wu C, Cui W, Wang L. DNA Methyltransferases in Cancer: Biology, Paradox, Aberrations, and Targeted Therapy. Cancers. 2020; 12: 2123.

[8] Wong KK, Lawrie CH, Green TM. Oncogenic Roles and Inhibitors of DNMT1, DNMT3A, and DNMT3B in Acute Myeloid Leukaemia. Biomarker Insights. 2019; 14: 1177271919846454.

[9] Lai SC, Su YT, Chi CC, Kuo YC, Lee KF, Wu YC, *et al*. DNMT3b/OCT4 expression confers sorafenib resistance and poor prognosis of hepatocellular carcinoma through IL-6/STAT3 regulation. Journal of Experimental & Clinical Cancer Research. 2019; 38: 474.

[10] Xu K, Chen B, Li B, Li C, Zhang Y, Jiang N, *et al*. DNMT3B silencing suppresses migration and invasion by epigenetically promoting miR-34a in bladder cancer. Aging. 2020; 12: 23668–23683.

[11] Li YF, Hsiao YH, Lai YH, Chen YC, Chen YJ, Chou JL, *et al*. DNA methylation profiles and biomarkers of oral squamous cell carcinoma. Epigenetics. 2015; 10: 229–236.

[12] Heawchaiyaphum C, Ekalaksananan T, Patarapadungkit N, Worawichawong S, Pientong C. Epstein-Barr Virus Infection Alone or Jointly with Human Papillomavirus Associates with Down-Regulation of miR-145 in Oral Squamous-Cell Carcinoma. Microorganisms. 2021; 9: 2496.

[13] Panchin AY, Makeev VJ, Medvedeva YA. Preservation of methylated CpG dinucleotides in human CpG islands. Biology Direct. 2016; 11: 11.

[14] Illingworth RS, Bird AP. CpG islands–'a rough guide'. FEBS Letters. 2009; 583: 1713–1720.

[15] Hughes AL, Kelley JR, Klose RJ. Understanding the interplay between CpG island-associated gene promoters and H3K4 methylation. Biochimica et Biophysica Acta. Gene Regulatory Mechanisms. 2020; 1863: 194567.

[16] Lee CH, Wong TS, Chan JYW, Lu SC, Lin P, Cheng AJ, *et al*. Epigenetic regulation of the X-linked tumour suppressors BEX1 and LDOC1 in oral squamous cell carcinoma. The Journal of Pathology. 2013; 230: 298–309.

[17] Notarstefano V, Belloni A, Sabbatini S, Pro C, Orilisi G, Monterubbianesi R, *et al*. Cytotoxic Effects of 5-Azacytidine on Primary Tumour Cells and Cancer Stem Cells from Oral Squamous Cell Carcinoma: An In Vitro FTIRM Analysis. Cells. 2021; 10: 2127.

[18] Nirgude S, Choudhary B. Insights into the role of GPX3, a highly efficient plasma antioxidant, in cancer. Biochemical Pharmacology. 2021; 184: 114365.

[19] Pedro NF, Biselli JM, Maniglia JV, Santi-Neto DD, Pavarino ÉC, Goloni-Bertollo EM, *et al*. Candidate Biomarkers for Oral Squamous Cell Carcinoma: Differential Expression of Oxidative Stress-Related Genes. Asian Pacific Journal of Cancer Prevention. 2018; 19: 1343–1349.

[20] Li LC, Dahiya R. MethPrimer: designing primers for methylation PCRs. Bioinformatics. 2002; 18: 1427–1431.

[21] Li KY, Zhang J, Jiang LC, Zhang B, Xia CP, Xu K, *et al*. Knockdown of USP39 by lentivirus-mediated RNA interference suppresses the growth of oral squamous cell carcinoma. Cancer Biomarkers: Section a of Disease Markers. 2016; 16: 137–144.

[22] Li S, Wu Y, Ding Y, Yu M, Ai Z. CerS6 regulates cisplatin resistance in oral squamous cell carcinoma by altering mitochondrial

Journal of
BIOLOGICAL REGULATORS
and Homeostatic Agents

fission and autophagy. Journal of Cellular Physiology. 2018; 233: 9416–9425.

[23] Yamada N, Nishida Y, Tsutsumida H, Goto M, Higashi M, Nomoto M, *et al*. Promoter CpG methylation in cancer cells contributes to the regulation of MUC4. British Journal of Cancer. 2009; 100: 344–351.

[24] Wang J, Xu P, Hao Y, Yu T, Liu L, Song Y, *et al*. Interaction between DNMT3B and MYH11 via hypermethylation regulates gastric cancer progression. BMC Cancer. 2021; 21: 914.

[25] Sun LP, Xu K, Cui J, Yuan DY, Zou B, Li J, *et al*. Cancer associated fibroblast derived exosomal miR 382 5p promotes the migration and invasion of oral squamous cell carcinoma. Oncology Reports. 2019; 42: 1319–1328.

[26] Livak KJ, Schmittgen TD. Analysis of relative gene expression data using real-time quantitative PCR and the 2(-Delta Delta C(T)) Method. Methods. 2001; 25: 402–408.

[27] Chen S, Li H, Li X, Chen W, Zhang X, Yang Z, *et al*. High SOX8 expression promotes tumor growth and predicts poor prognosis through GOLPH3 signaling in tongue squamous cell carcinoma. Cancer Medicine. 2020; 9: 4274–4289.

[28] Li MH, Liao X, Li C, Wang TT, Sun YS, Yang K, *et al*. Lycorine hydrochloride induces reactive oxygen species-mediated apoptosis via the mitochondrial apoptotic pathway and the JNK signaling pathway in the oral squamous cell carcinoma HSC-3 cell line. Oncology Letters. 2021; 21: 236.

[29] Zhang ZM, Lu R, Wang P, Yu Y, Chen D, Gao L, *et al*. Structural basis for DNMT3A-mediated de novo DNA methylation. Nature. 2018; 554: 387–391.

[30] Wang JC, Wang Z, Fan YX, Si YQ, Wang JX. DNA methyltransferase 3b silencing affects locus-specific DNA methylation and inhibits proliferation, migration and invasion in human hepatocellular carcinoma SMMC-7721 and BEL-7402 cells. Oncology Letters. 2015; 9: 2499–2506.

[31] Roll JD, Rivenbark AG, Jones WD, Coleman WB. DNMT3b overexpression contributes to a hypermethylator phenotype in human breast cancer cell lines. Molecular Cancer. 2008; 7: 15.

[32] Chen WC, Chen MF, Lin PY. Significance of DNMT3b in oral cancer. PLoS ONE. 2014; 9: e89956.

[33] Shiah SG, Hsiao JR, Chang HJ, Hsu YM, Wu GH, Peng HY, *et al*. MiR-30a and miR-379 modulate retinoic acid pathway by targeting DNA methyltransferase 3B in oral cancer. Journal of Biomedical Science. 2020; 27: 46.

[34] Horii T, Hatada I. Regulation of CpG methylation by Dnmt and Tet in pluripotent stem cells. The Journal of Reproduction and Development. 2016; 62: 331–335.

[35] Ku JL, Jeon YK, Park JG. Methylation-specific PCR. Methods in Molecular Biology. 2011; 791: 23–32.

[36] Worley BL, Kim YS, Mardini J, Zaman R, Leon KE, Vallur PG, *et al*. GPx3 supports ovarian cancer progression by manipulating the extracellular redox environment. Redox Biology. 2019; 25: 101051.

[37] Pelosof L, Yerram S, Armstrong T, Chu N, Danilova L, Yanagisawa B, *et al*. GPX3 promoter methylation predicts platinum sensitivity in colorectal cancer. Epigenetics. 2017; 12: 540–550.

[38] Cai M, Sikong Y, Wang Q, Zhu S, Pang F, Cui X. Gpx3 prevents migration and invasion in gastric cancer by targeting NFκB/Wnt5a/JNK signaling. International Journal of Clinical and Experimental Pathology. 2019; 12: 1194–1203.

[39] Han L, Yang X, Sun W, Li Z, Ren H, Li B, *et al*. The study of GPX3 methylation in patients with Kashin-Beck Disease and its mechanism in chondrocyte apoptosis. Bone. 2018; 117: 15–22.

[40] Xu Y, Li Z, Huai T, Huo X, Wang H, Bian E, *et al*. DNMT1 Mediated CAHM Repression Promotes Glioma Invasion via SPAK/JNK Pathway. Cellular and Molecular Neurobiology. 2022; 42: 2643–2653.

[41] Zeke A, Misheva M, Reményi A, Bogoyevitch MA. JNK Signaling: Regulation and Functions Based on Complex Protein-Protein Partnerships. Microbiology and Molecular Biology Reviews. 2016; 80: 793–835.

[42] Kumar A, Singh UK, Kini SG, Garg V, Agrawal S, Tomar PK, *et al*. JNK pathway signaling: a novel and smarter therapeutic targets for various biological diseases. Future Medicinal Chemistry. 2015; 7: 2065–2086.

[43] Li B, Zhou P, Xu K, Chen T, Jiao J, Wei H, *et al*. Metformin induces cell cycle arrest, apoptosis and autophagy through ROS/JNK signaling pathway in human osteosarcoma. International Journal of Biological Sciences. 2020; 16: 74–84.